

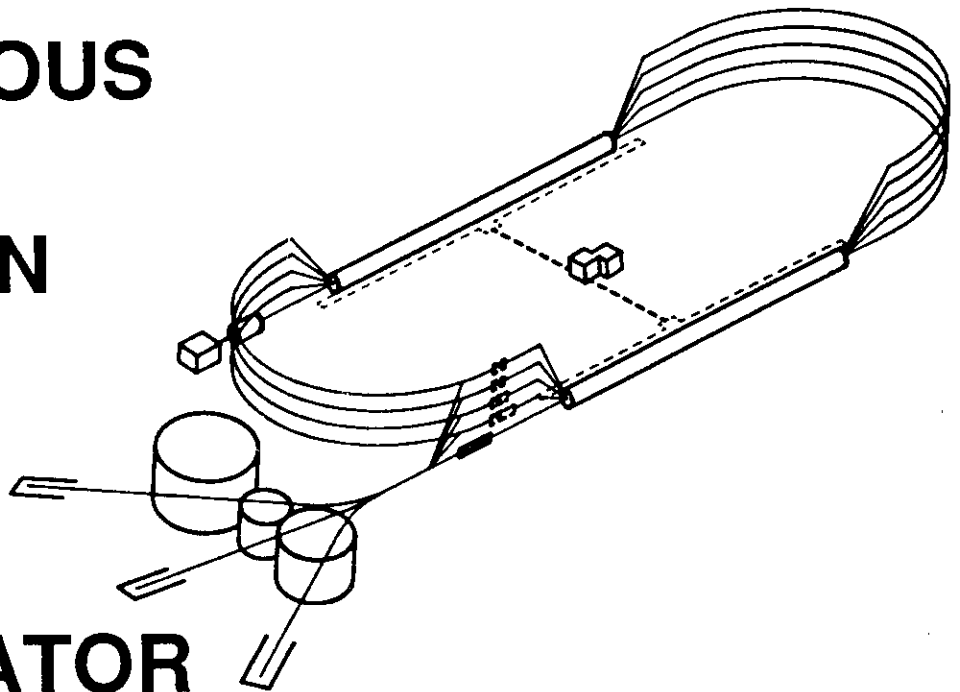
June 30, 1993

Spin Structure Functions of the Nucleon at Low Q^2 and ν^*

Volker D. Burkert
*CEBAF, 12000 Jefferson Avenue, Newport News,
Virginia 23606, USA*

***Invited talk presented at the 6th International Workshop on Perspectives
in Intermediate Energy Nuclear Physics, Trieste, May 4-7, 1993.**

CONTINUOUS
ELECTRON
BEAM
ACCCELERATOR
FACILITY



SURA *Southeastern Universities Research Association*

CEBAF
The Continuous Electron Beam Accelerator Facility
Newport News, Virginia

Copies available from:

Library
CEBAF
12000 Jefferson Avenue
Newport News
Virginia 23606

The Southeastern Universities Research Association (SURA) operates the Continuous Electron Beam Accelerator Facility for the United States Department of Energy under contract DE-AC05-84ER40150.

DISCLAIMER

This report was prepared as an account of work sponsored by the United States government. Neither the United States nor the United States Department of Energy, nor any of their employees, makes any warranty, express or implied, or assumes any legal liability or responsibility for the accuracy, completeness, or usefulness of any information, apparatus, product, or process disclosed, or represents that its use would not infringe privately owned rights. Reference herein to any specific commercial product, process, or service by trade name, mark, manufacturer, or otherwise, does not necessarily constitute or imply its endorsement, recommendation, or favoring by the United States government or any agency thereof. The views and opinions of authors expressed herein do not necessarily state or reflect those of the United States government or any agency thereof.

Spin Structure Functions of the Nucleon at low Q^2 and ν *

Volker D. Burkert
 CEBAF, 12000 Jefferson Avenue, Newport News,
 Virginia 23606, USA

ABSTRACT

Phenomenological approaches to describe the spin structure functions and spin sum rules for proton and neutrons at low momentum transfer Q^2 and energy transfer ν , i.e. in the region of the nucleon resonances are discussed. Experiments to measure A_1^p , A_2^p and A_1^n structure functions at CEBAF in a Q^2 range from 0.15 to 2.0 GeV^2 , and a W range from threshold to 2.2 GeV are presented.

1. Introduction

The results of the EMC measurements¹ on the polarized proton structure functions have prompted numerous speculations about whether or not in the deep-inelastic region the spin of the proton is carried by the quarks. Recent results from the CERN Spin Muon collaboration (SMC)² and SLAC experiment E142³ on the neutron polarized structure functions added additional speculations as in one interpretation the neutron spin is not carried by quarks either, whereas in another interpretation, the (fundamental) Björken sum rule⁴ would be violated while leaving the (less fundamental) Ellis-Jaffe sum rule⁵ for the neutron intact. It is worth noting that the experiments on the neutron use data sets with Q^2 as low as 1 GeV^2 . While such low Q^2 values have been used in the analysis of unpolarized lepton scattering there is a lack of convincing evidence that polarized structure functions exhibit true scaling behavior at such low Q^2 . One should also keep in mind that the various spin sum rules are only defined for fixed Q^2 while the experiments integrate over large ranges in Q^2 . Moreover, the W range used in these analyses ($W \geq 2 \text{ GeV}$) may overlap part of the resonance region. The general perception appears to be that for $W \geq 2 \text{ GeV}$ one probes the deep inelastic and hence scaling regime. However, even in the deep inelastic regime one should observe a scale breaking Q^2 dependence. Moreover, excited nucleon states with masses as high as 3.0 GeV have been observed, and many states are predicted to exist in the mass region above 2.0 GeV , which raises the interesting question of how to correct for contributions resulting from these states. As the conclusion about the spin of the proton not being carried by quarks rests on relatively small differences between theoretical predictions and the data it is important to study such contributions before far-reaching conclusions about the origin of the nucleon spin may be drawn.

In some interpretations of the EMC results it is assumed that the missing quark spin may be accounted for by the so-called axial anomaly.⁶ However, such contributions are rather controversial.⁷ If the entire effect is attributed to these contributions gluons would have to account for about 600% of the proton spin; most of it would have to be compensated by contributions from orbital angular momenta. Another possibility is that most of the proton spin resides in orbital angular momentum contributions. Such contributions are necessarily associated with extended objects and therefore cannot be probed in deep inelastic scattering, but they may be accessible at lower energies and momentum transfers. The low Q^2 , ν region may therefore contain significant information about the spin structure of the nucleon.

In this talk I will discuss some aspects of polarized structure functions of the nucleon in the non-perturbative regime: low four momentum transfer Q^2 and low energy transfer ν . This is the kinematical regime where contributions from excited N^* and Δ^* resonances may be important.

2. Polarized Structure Functions of the Proton

The spin-structure of the proton is usually discussed in relation to the deep-inelastic polarized structure functions $g_1(x)$. In the kinematical regime of resonances and low Q^2 use of total helicity 1/2 and 3/2 photon-nucleon absorption cross sections is more convenient.

The double polarized inclusive electron scattering cross section may be written as:

$$\frac{d\sigma}{d\Omega dE'} = \Gamma_T \{ \sigma_T + \epsilon \sigma_L \pm \sqrt{1 - \epsilon^2} \cos \psi \sigma_T A_1 \pm \sqrt{2\epsilon(1 - \epsilon)} \sin \psi \sigma_T A_2 \} \quad (1)$$

σ_T and σ_L are the transverse and longitudinal total photon absorption cross section, and the sign \pm is related to the sign of the product of beam and target polarization (assumed to be unity). A_1 and A_2 are the polarized asymmetries:

$$A_1 = \frac{\sigma_{1/2}^T - \sigma_{3/2}^T}{\sigma_{1/2}^T + \sigma_{3/2}^T} \quad (2)$$

$$A_2 = \frac{\sigma^{TL}}{\sigma_{1/2}^T + \sigma_{3/2}^T} \quad (3)$$

where $\sigma_{1/2}^T(Q^2, \nu)$ and $\sigma_{3/2}^T(Q^2, \nu)$ are the transverse total absorption cross sections for total helicity $\lambda_{\gamma N} = 1/2$ and $\lambda_{\gamma N} = 3/2$, respectively. A_1 is limited to:

$$-1 \leq A_1 \leq +1 ,$$

and A_2 is a transverse-longitudinal interference term with an upper bound of:

$$A_2 \leq \sqrt{\frac{\sigma_L}{\sigma_T}} \quad (4)$$

At $Q^2 = 0$ the sum rule by Gerasimov,⁸ and Drell and Hearn⁹ relates the difference in the total photoabsorption cross section on nucleons for $\lambda_{\gamma N} = 1/2$ and $\lambda_{\gamma N} = 3/2$ to the anomalous magnetic moment of the target nucleon.

$$I_p(0) = \frac{M_p^2}{8\pi^2\alpha} \int_{\nu_{\text{thr}}}^{\infty} \frac{d\nu}{\nu} (\sigma_{1/2}^p(\nu) - \sigma_{3/2}^p(\nu)) = -\frac{1}{4}\kappa^2 \quad (5)$$

Assuming scaling behavior the EMC results can be extrapolated to lower Q^2

$$I_p(Q^2) = \frac{2M_p^2}{Q^2} \Gamma_p^{EMC} \simeq \frac{0.222 \pm 0.018 \pm 0.026}{Q^2} \quad (6)$$

where QCD corrections have been neglected.

Note that $I_p(0)$ is large and negative, whereas the EMC data yield a positive $I_p(Q^2)$. In order to reconcile the GDH sum rule with the EMC results, dramatic changes in the helicity structure must occur when going from $Q^2 = 0$ to finite values of Q^2 . This is illustrated in Fig. 1. In an analysis of photoproduction data by Karliner¹⁰ and recently by Workman and Arndt¹¹ for energies up to $E_\gamma = 1.7 \text{ GeV}$ single pion production contributions were found to nearly saturate the sum rule. An analysis of electroproduction data by Burkert and Li¹² including all known resonant channels as well as non-resonant single pion Born terms showed that contributions of the $\Delta(1232)$ to $I_p(Q^2)$ are dominant at small Q^2 . This analysis also showed that contributions from other resonances become significant with increasing Q^2 , in fact causing $I_p(Q^2)$ to change its sign at Q^2 between 0.5 to 1.0 GeV^2 . It is interesting to note that resonance contributions other than the $\Delta(1232)$ contribute as much as 50% or more of the extrapolated EMC results at $Q^2 = 1 \text{ GeV}^2$ (Fig. 2). Anselmino et al.¹³ attempted to connect the GDH sum rule with the Ellis-Jaffe sum rule in the deep inelastic region using the vector dominance

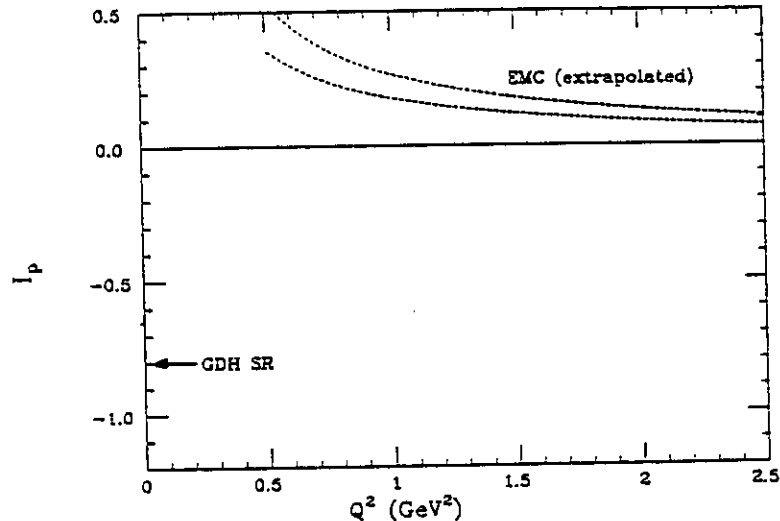


Figure 1: The integral $I_p(Q^2)$ extrapolated from the EMC data assuming a $1/Q^2$ behavior (area between dashed lines). The arrow at $Q^2 = 0$ indicates the GDH sum rule value.

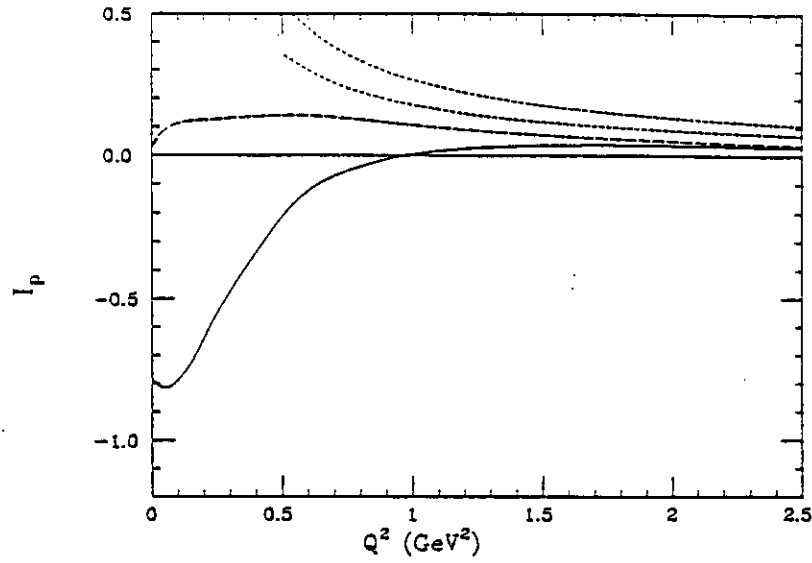


Figure 2: The integral $I_p(Q^2)$. The solid curve represents the results of the empirical analysis by Burkert and Li.¹² The long dashed line is the result of the same analysis excluding the $\Delta(1232)$ contribution. The short dashed lines represent the extrapolated EMC results.

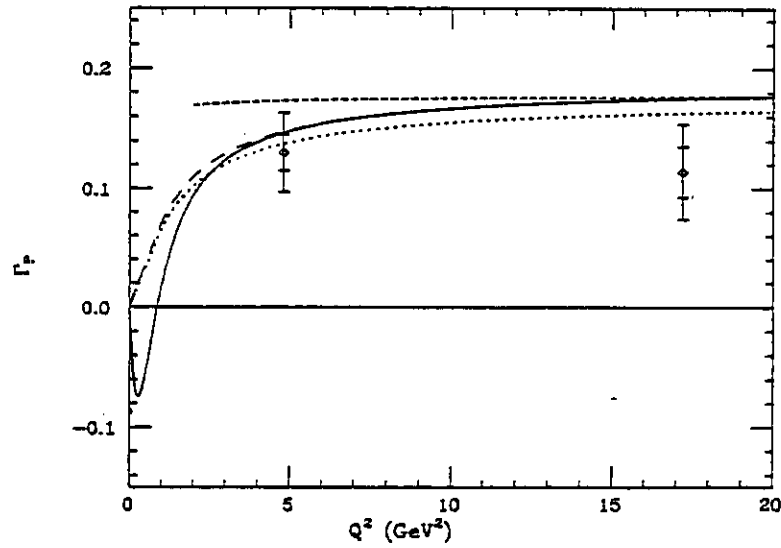


Figure 3: $\Gamma_p(Q^2)$ using eqn.(7) (solid line), with $\Gamma_p^{as} = \Gamma_p^{EJ}$, note: $\Gamma_p = (Q^2/2M_p^2)I_p$. The EMC data are shown with their statistical and systematic errors. The short dashed line is the EJ sum rule.

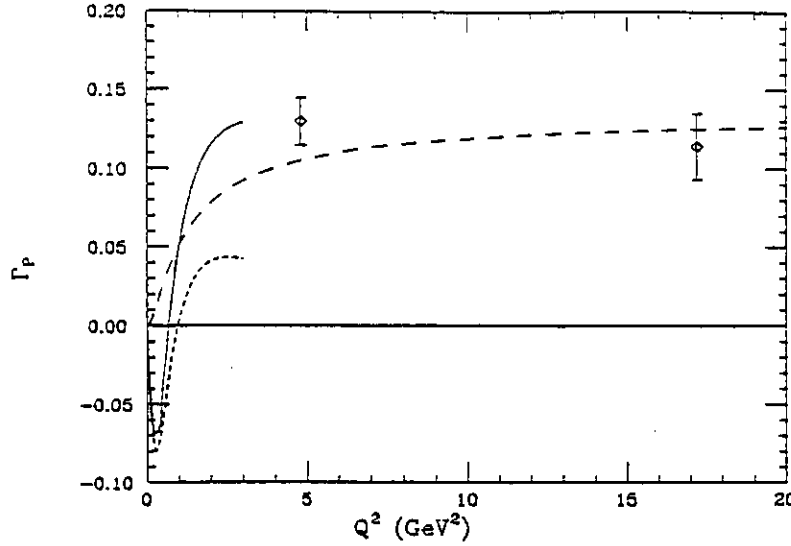


Figure 4: Same as in Fig. 3, but with all resonances included (solid line), and with $\Gamma_p(Q^2 = 10.7 \text{ GeV}^2) = 0.126$ according to the EMC results. Short dashes include resonances only, long dashes represent VDM contributions.

analogy. The resulting strong Q^2 dependence was found to be in disagreement with the EMC data. Burkert and Ioffe¹⁴ extended this model to include contributions from the $\gamma_v N \Delta$ transition, the asymptotic value being fixed to the original Ellis-Jaffe sum rule:

$$I_p(Q^2) = I_{p\Delta}(Q^2) + 2M_p^2 \Gamma_p^{as} \left[\frac{1}{Q^2 + m_\rho^2} - \frac{cm_\rho^2}{(Q^2 + m_\rho^2)^2} \right] \quad (7)$$

The parameter c is fixed to $c = 1.05$ by requiring $I_p(0) = I_p^{GDH}$. From this, significant contributions from high twist or Δ contributions may be present at $Q^2 \leq 4 \text{ GeV}^2$ (Fig. 3). When higher resonances are included (Fig. 4) the deviations from scaling behavior set in at $Q^2 \leq 2 \text{ GeV}^2$, whereas at higher Q^2 , resonant and high twist contributions appear to conspire to generate a ‘scaling-like’ behavior: in this analysis $\Gamma_p^{as} = 0.134$ was assumed in accordance with the EMC results. Unfortunately, for $Q^2 \geq 3 \text{ GeV}^2$ resonance excitations have not been measured, however, assuming a smooth falloff for the resonance contributions with Q^2 , an approximate scaling behavior will be the result. Further theoretical studies will be required to understand in what way such a behavior will affect the interpretation of the polarized structure function measurements.

3. Polarized Structure Functions of the Neutron

The GDH sum rule for the neutron is of special interest for testing the quark model. In the $SU(6) \otimes O(3)$ basis the GDH sum rule obtains contributions from the $\gamma N \Delta(1232)$ transition only¹⁵:

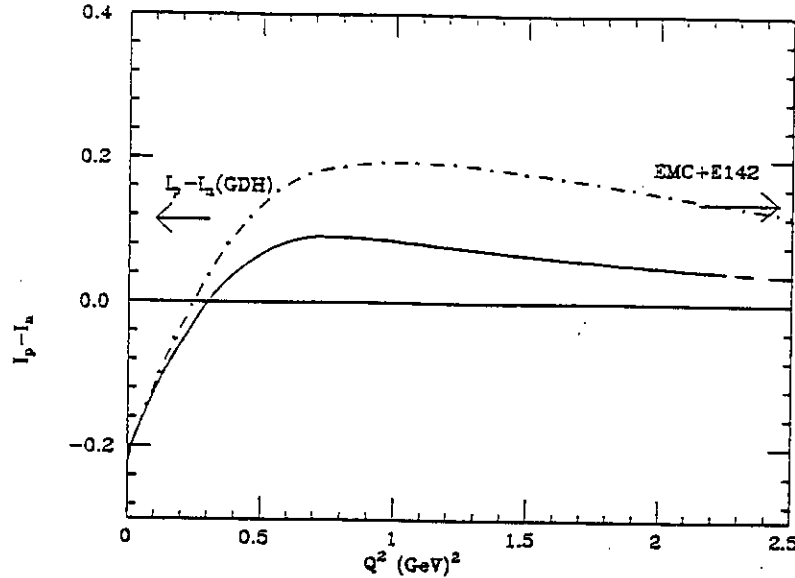


Figure 5: Result of the analysis of electroproduction of baryon resonances for the proton - neutron difference if only resonances are included using the AO code.¹⁶ The $P_{11}(1440)$ is assumed to be a (q^3) state in the nonrelativistic quark model (dashed-dotted), or as a (q^3G) hybrid state¹⁷ (solid)

$$I_n^{GDH}(Q^2) = I_n^{\Delta(1232)}(Q^2)$$

This prediction is based on the symmetry properties of the quark model; a deviation would indicate a breaking of the $SU(6) \otimes O(3)$ symmetry and demonstrate the limitations of the nonrelativistic quark model. The proton-neutron difference $\Delta I_{pn}(Q^2)$ as a function of Q^2 allows the study the transition from the Björken sum rule, which is expected to be valid in the deep inelastic region, to the GDH sum rule at $Q^2 = 0$. Since in ΔI_{pn} the dominant $\Delta(1232)$ contribution is absent, such a measurement will be sensitive to isospin 1/2 resonance contributions, most notably to the lowest mass state $P_{11}(1440)$. The 3-quark nature of this state has been disputed for some time. Calculations of transition form factors assuming it is a gluonic excitation¹⁷ of the nucleon rather than a radial 3-quark excitation give better agreement with the experimental amplitudes. As shown in Fig. 5, measurements of ΔI_{pn} are sensitive to the QCD structure of this state. This is because in this integral the dominant contribution of the $\Delta(1232)$ to I_p and I_n cancel. The GDH value is $\Delta I_{pn}(0) = +0.114$. The analysis¹¹ of single pion photoproduction data yields $\Delta I_{pn} \sim -0.267$, consistent with the analysis of electroproduction data¹² (Fig. 5) which yield - 0.211 for resonance contributions, and - 0.365 if single pion Born terms are included as well. The data indicate significant discrepancies with the GDH sum rule. However, this discrepancy may be just an artifact of the limited kinematical range included in the analysis. In particular, data on neutrons are quite sparse, and the analysis has to rely largely on single quark transition symmetry arguments to determine the amplitudes for many of the higher mass states.

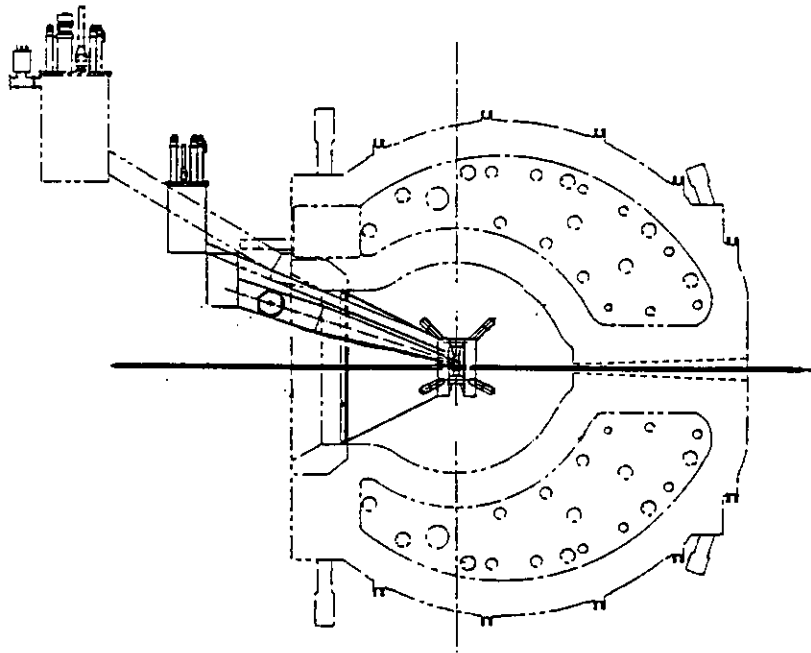


Figure 6: Experimental arrangement of the CEBAF experiment 91-023. The target is polarized parallel or anti-parallel to the beam axis.

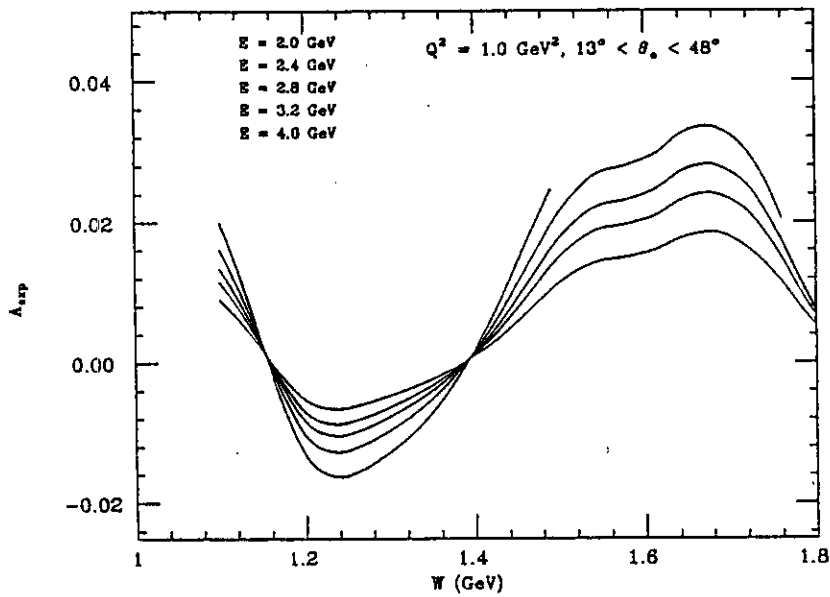


Figure 7: Expected experimental asymmetries for different beam energies but fixed Q^2 and W . A fit of eqn.(8) to A at different energies allows to separate A_1 and A_2 .

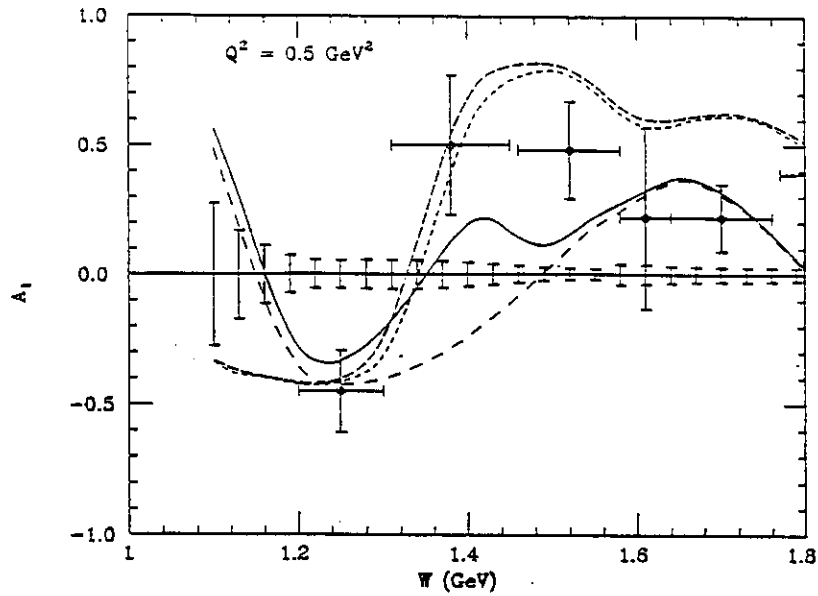


Figure 8: Expected statistical errors in experiment 91-023¹⁹ for asymmetry $A_1(Q^2, W)$ compared with SLAC/Yale data.²⁰

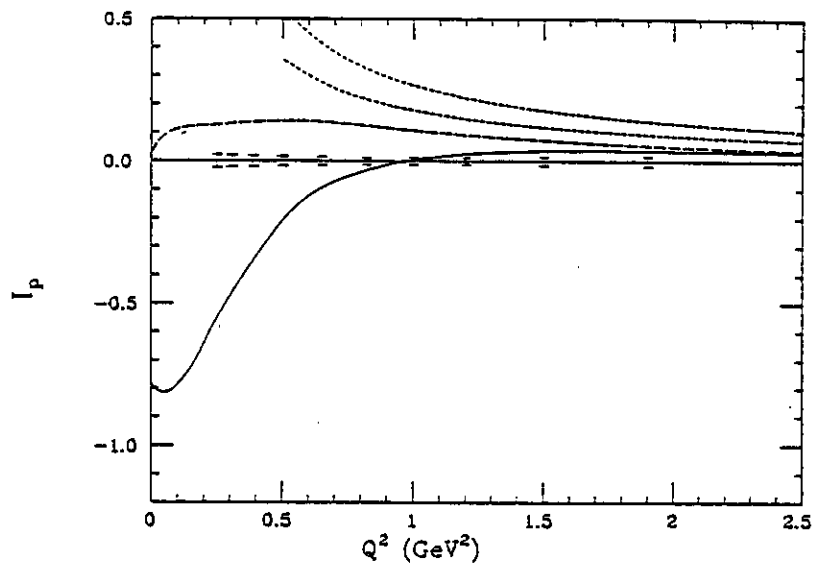


Figure 9: Expected errors for $I_p(Q^2)$ from experiment 91-023.¹⁹

A violation of the GDH sum rule would be quite significant. In recent theoretical work on extended algebra¹⁸ it is suggested that the GDH sum rule needs to be extended since one of its basic assumptions, the existence of one pole only, may not be correct. Interestingly enough, the discrepancy observed in the empirical analyses is qualitatively consistent with this prediction.

4. Experiments at CEBAF

Experiment 91-023¹⁹ will use the CEBAF Large Acceptance Spectrometer²¹ to measure the asymmetries $A_1^p(Q^2, \nu)$, and $A_2^p(Q^2, \nu)$. The experimental arrangement is shown in Fig. 6, where the $^{15}\text{NH}_3$ target will be polarized along the beam axis. In order to separate A_1 and A_2 the experimental asymmetry

$$A \equiv \frac{\frac{d\sigma(\uparrow\downarrow)}{d\Omega dE'} - \frac{d\sigma(\uparrow\uparrow)}{d\Omega dE'}}{\frac{d\sigma(\uparrow\downarrow)}{d\Omega dE'} + \frac{d\sigma(\uparrow\uparrow)}{d\Omega dE'}} = P_e \cdot P_p \cdot D[A_1(Q^2, \nu) + \eta A_2(Q^2, \nu)] \quad (8)$$

$$D = \frac{\sqrt{1 - \epsilon^2} \cos \psi}{1 + \epsilon R}; \quad \eta = \sqrt{\frac{2\epsilon}{1 + \epsilon}} \tan \psi$$

will be measured at fixed Q^2 and W but at different beam energies, giving different values for η . ψ is the angle between the polarization axis and the direction of the photon. The experiment will measure the angular range for about 13° to 48° over most of the azimuthal angle range simultaneously. The solid angle covered is $\Delta\Omega = 1.2$ sr. In the asymmetry many systematic uncertainties, e.g. due to limited knowledge of the acceptance, will cancel. Systematic uncertainty due to the limited knowledge of beam and target polarization will be greatly reduced by measuring the elastic asymmetry

$$A_{ep} = P_e \cdot P_p \cdot f(G_E/G_M), \quad (9)$$

simultaneously. A_{ep} is a function of the ratio of electric and magnetic form factors, and the product of beam and target polarization. Since the form factors are known at small Q^2 very accurately, $P_e \cdot P_p$ can be determined to $\delta(P_e \cdot P_p) \leq 0.01$. Fig. 7 shows expected experimental asymmetries for different beam energies. A fit of eqn(8) at fixed Q^2 and W will allow the determination of A_1 and A_2 , separately. Expected error bars for the asymmetries are shown in Fig. 8, where data previously measured by a SLAC/Yale experiment at $Q^2 = 0.5 \text{ GeV}^2$ are included for comparison. Asymmetries for 10 values of Q^2 between 0.15 GeV^2 and 2 GeV^2 will be measured. In case A_2 is known from some other source, e.g. from an analysis of unpolarized pion electroproduction data, A_1 can be determined with considerably reduced error bars. The integral

$$I_p(Q^2) = \int_{\nu_{thr}}^{\nu(W \leq 2 \text{ GeV})} 2\sigma_T A_1 \frac{d\nu}{\nu} \quad (10)$$

will be determined with statistical errors as shown in Fig. 9.

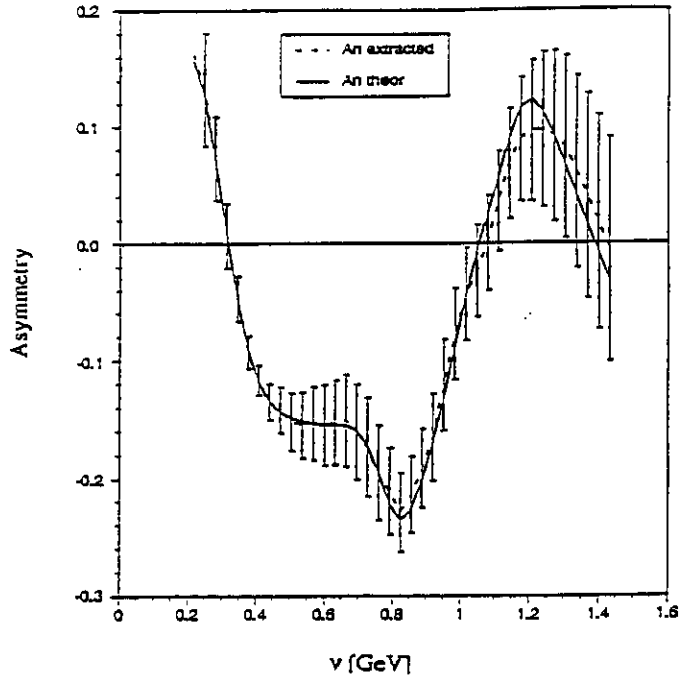


Figure 10: Expected statistical error for the asymmetry $A/D(e\pi) \cdot \sigma_T$. The deviations of the expected data points from the line indicate the systematic uncertainty due to the assumption $A_2^n = 0$.

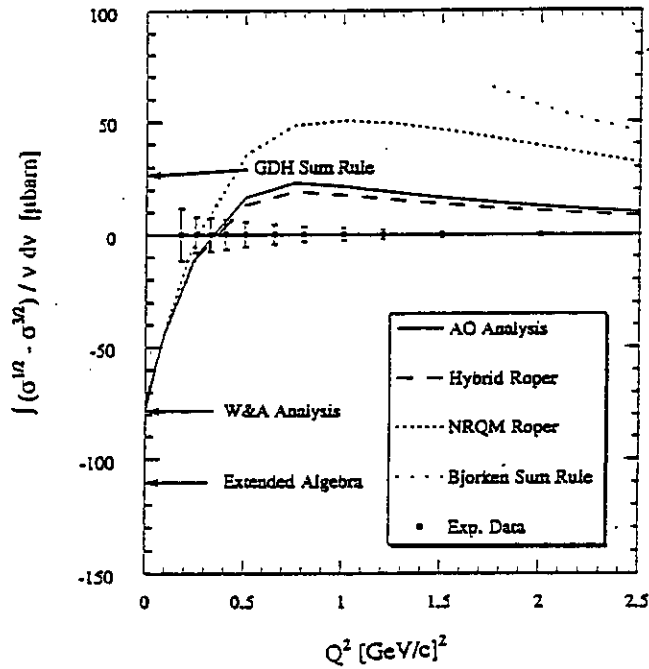


Figure 11: Expected errors for the proton - neutron difference $\Delta I_{pn}(Q^2)$.

$$\int A_t(\theta, \phi) P_1(\theta) \sin(\phi) d\Omega$$

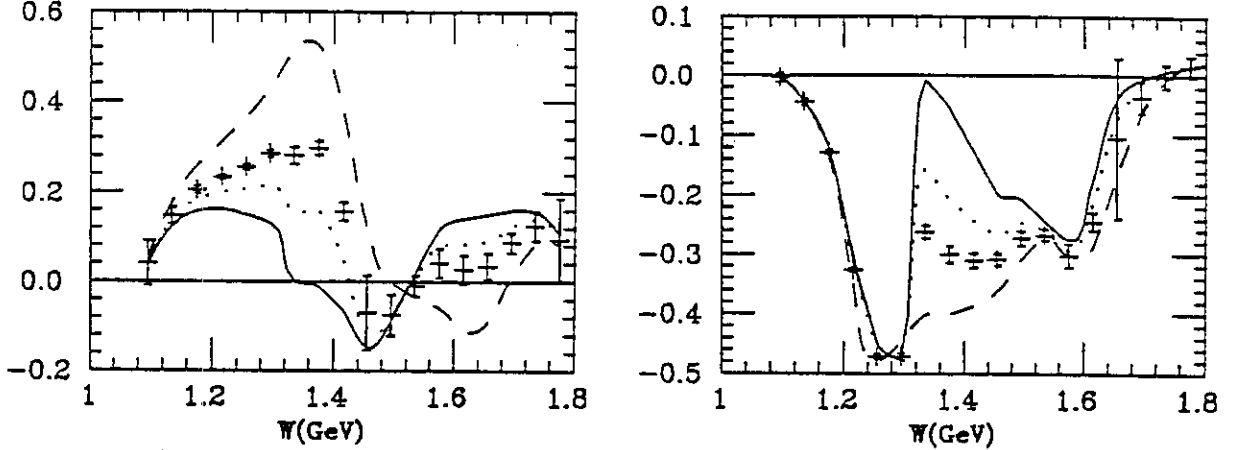


Figure 12: Moments of the polarized target asymmetry for single π^0 (left) and π^+ production. The curves represent results using the AO code¹⁶ for various models of the $P_{11}(1440)$ structure. Also shown are projected error bars for the experiment.

5. Measurement on the Neutron.

In another experiment²² the GDH sum rule for deuterium will be measured. The two experiments will allow extraction of the neutron GDH sum rule as well as the proton-neutron difference ΔI_{pn} . Calculations using the AO code¹⁶ show that for the neutron, A_2^n may be small, and one can extract A_1^n from eqn. (8) assuming $A_2^n = 0$. Figure 10 shows the expected errors for the experimental asymmetry $(A/D)\sigma_T$ on the neutron. Obviously, a very significant determination of $\Delta I_{pn}(Q^2)$ will be possible (Fig. 11), allowing tests of the validity of the GDH sum rule for isospin 1/2 contributions.

6. Exclusive Polarized Proton Asymmetries

Experiment 93-036²³ will measure polarization observables in single pion production. This experiment, in conjunction with the unpolarized experiments of the N^* program²⁴ will allow to isolate helicity transition amplitudes $A_{1/2}$, $A_{3/2}$ for individual resonances throughout the entire resonance region. The Q^2 dependence of $A_{1/2}$, $A_{3/2}$ will reveal the QCD structure of resonant states. For example, the transverse $A_{1/2}(Q^2)$ and the longitudinal $S_{1/2}$ amplitudes for the $P_{11}(1440)$ are very sensitive to internal quark-gluon structure: (q^3) state versus (q^3G) state. As an illustrative example Fig. 12 shows first moments of the polarized target asymmetries for various models of the structure of the $P_{11}(1440)$. Measurement of $A_{1/2}$, $A_{3/2}$ for states with $J \geq 3/2$ will

allow the determination of helicity asymmetries:

$$A_1^{res} = \frac{\sigma_{1/2}^T - \sigma_{3/2}^T}{\sigma_{1/2}^T + \sigma_{3/2}^T} = \frac{A_{1/2}^2 - A_{3/2}^2}{A_{1/2}^2 + A_{3/2}^2} \quad (11)$$

for these states. It will therefore be possible to determine the contributions of individual states to the GDH integral. In comparison with quark model calculations it may be possible to identify the quark spin content of the resonance transition.

7. Summary

Measurement of polarized structure functions of the proton and neutron at low Q^2 and ν allows tests of the validity of the GDH sum rule. Phenomenological analyses of pion photo- and electroproduction yield significant discrepancies with the GDH sum rule for the proton/neutron difference. The measurements will also provide tests of models of the nucleon structure. The significance of these measurements for the interpretation of the deep inelastic polarized structure functions should be examined theoretically in detail.

References

1. J. Ashman et al., *Phys. Lett.* B206 (1988)364; *Nucl. Phys.*B328 (1989)1.
2. B. Adeva et al., *Phys. Lett.* B 302 533 (1993); also: T.O. Niinikoski, talk at this conference.
3. S. Rock, talk at this conference.
4. J.D. Björken, *Phys.Rev.*148, 1467(1966).
5. J. Ellis and R.L. Jaffe, *Phys. Rev.* D9, 1444 (1974)
6. G. Altarelli, G.G. Ross, *Phys. Lett.* B214, 381(1988); R. Carlitz, J.C. Collins, A.M. Mueller, *Phys. Lett.*B214, 2229 (1988)
7. R. Manohar, in: *Polarized Collider Workshop, University Park, Pa. , 1990., AIP Conference Proc. No.223.*
8. S. Gerasimov, *Yad.Fiz.*2, 598(1965) [*Sov. J. Nucl. Phys.*2 (1966)930.
9. S.D. Drell and A.C. Hearn, *Phys. Rev. Lett.* 16 (1966) 908.
10. I. Karliner, *Phys.Rev.* D7, 2717 (1973)
11. R. Workman and R. Arndt, *Phys. Rev.* D45, 1789(1992)
12. V. Burkert and Zh. Li, *Phys. Rev.*D47, 46(1993)
13. M. Anselmino, B.L. Ioffe and E. Leader, *Sov. J. Nucl. Phys.* 49 (1989) 136.
14. V. Burkert and B.L. Ioffe, *Phys. Lett.*B296 (1992)223
15. I.G. Aznauryan, *Yad. Fiz.* 6, 124(1966) [*Sov. J. Nucl. Phys.* 6, 91(1967)]; Z.P. Li, *Phys.Rev.*D47, 1854(1993).
16. V. Burkert and Zh. Li, *Computer code AO (unpublished).*
17. Z.P. Li, V. Burkert, Zh. Li, *Phys. Rev.* D46, 70(1992).
18. L.N. Chang, Y.G. Liang and R. Workman, (unpublished)
19. V. Burkert, D. Crabb, R. Minehart et al., *CEBAF Proposal 91-023.*
20. G. Baum et al., *Phys.Rev. Lett.* 45, 2000 (1980).

21. V. Burkert and B. Mecking, in: 'Modern Topics in Electron Scattering', in: *World Scientific, 1991*; eds. B. Frois and I. Sick.
22. S. Kuhn et al., *CEBAF Proposal 93-009*.
23. H. Weller, R. Chasteler and R. Minehart et al., *CEBAF proposal 93-036*.
24. CEBAF N* program; *Proposals 89-037, -038, -039, -040, -042, -043, 91-024*.